Supplementary Information (SI) for Journal of Materials Chemistry C.
This journal is © The Royal Society of Chemistry 2024

Electronic Supplementary Information

Journal of Materials Chemistry C

Greenish yellow-emitting carbon dot-based films for luminescent solar concentrator applications

Yunxiang Liu, Yoshiki Iso* and Tetsuhiko Isobe*

Department of Applied Chemistry, Faculty of Science and Technology, Keio University, 3-14-1 Hiyoshi, Kohoku-ku, Yokohama 223-8522, Japan

*Corresponding authors.

Yoshiki Iso – E-mail: iso@applc.keio.ac.jp; Tel.: +81 45 566 1558; Fax: +81 45 566 1551; orcid.org/0000-0001-7483-2828

Tetsuhiko Isobe – E-mail: isobe@applc.keio.ac.jp; Tel.: +81 45 566 1554; Fax: +81 45 566 1551; orcid.org/0000-0002-0868-5425

Table S1 Information of various carbon dots (CDs) in luminescent solar concentrators (LSCs).

Carbon source	Synthesis Method	Purification	λ_{em} (nm)	PLQY	Year	Ref.
Citric acid, urea	160/200 °C, 6 h in dimethylformamide (Solvothermal)	Dialysis/ Cold precipitation	500-600	40% / 20-30% in methanol/hexane	2018	S1
o-Phenylenediamine, L-tyrosine/dopamine	200 °C, 8 h in water (Hydrothermal)	Filtration, evaporation, dialysis	555-594/ 650	86.4% / 17.6% in methanol	2021	S2
Citric acid, dicyandiamide, 3-aminopropyltriethoxysilane	200 °C, 12 h in a mixture of ethanol and water (Solvothermal)	Centrifugation, washing with water and ethanol	517	49% in organosilicon matrix	2022	S3
Citric acid, urea	Microwave heating, 5 min, in water	Filtration	500-562	-	2017	S4
Citric acid, urea	Microwave heating, 5 min, in water	Filtration	420-560	80% in water	2018	S5
Nitrated pyrenes, boric acid / citric acid, urea, $CaCl_2$	180 °C, 12 h in Dimethylformamide / Gradually heated to 250 °C under vacuum (Solvothermal)	Centrifugation, redispersion / Centrifugation, dialysis, drying,	550-700 / 450-650	65% in toluene / -	2023	S6
Citric acid, urea, $CaCl_2$	Microwave heating, 2-6 min	Filtration, centrifugation, dialysis	406-550	15-73% in ethanol	2024	S7
Citric acid, L-cysteamine hydrochloride / Citric acid, urea / 1,3,5-Benzenetricarboxylic acid, 3,4,9,10-perylenetetracarboxylic dianhydride	Vacuum heating/Solvothermal	Silica gel chromatography, dialysis	495 / 516 / 584	90-72% in ethanol	2024	S8
Citric acid, urea, $CaCl_2$	Space-confined vacuum heating	Centrifugation, dialysis	500	65% in methanol	2021	S9
p-Phenylenediamine	250 °C, 12 h in diphenyl ether (Ambient air heating)	Centrifugation and silica gel column chromatography	540	56% / 30-56% in chloroform / ethylene-vinyl acetate copolymer		This work

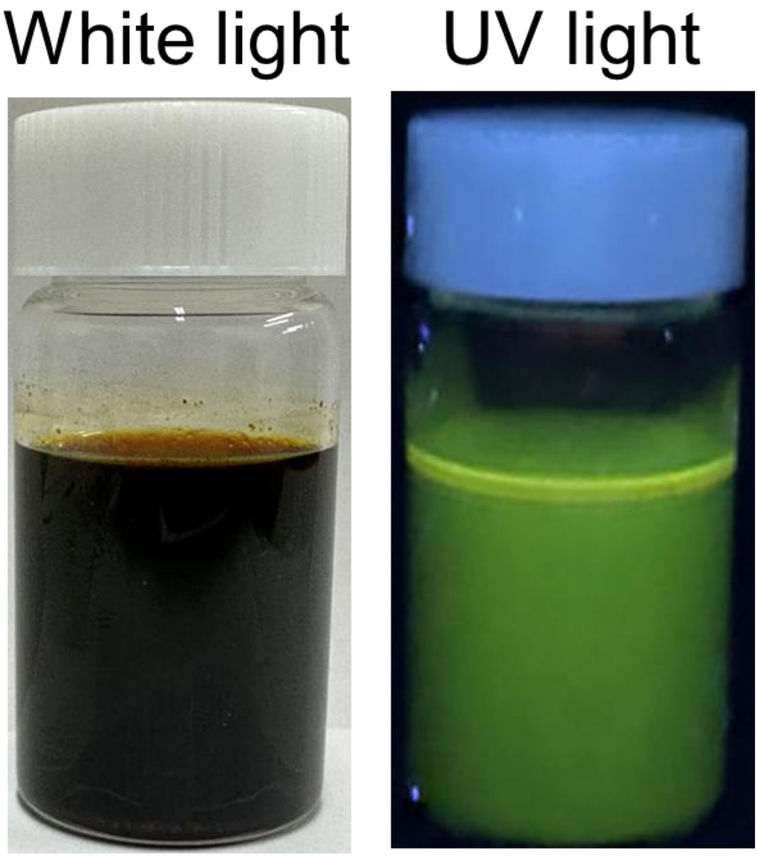

Fig. S1 Photographs of black suspension under white light and 365 nm UV light.

Crude CDs : 154 mg Purified CDs : 50 mg

Fig. S2 Photographs of crude CDs and purified CDs

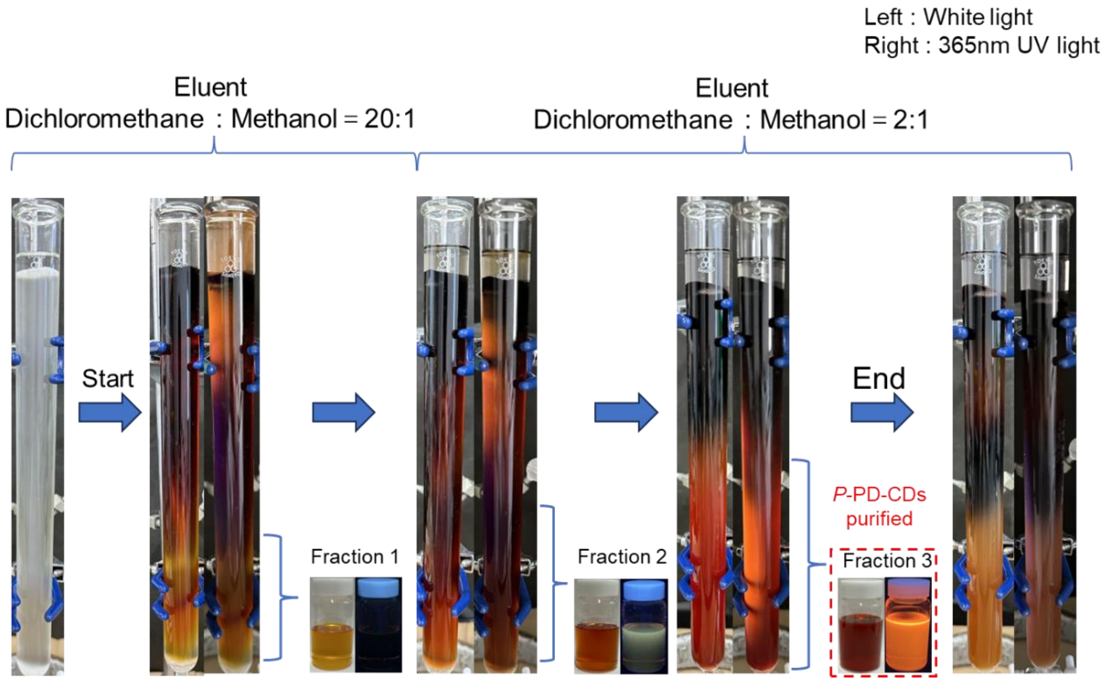

Fig. S3 Purification of crude CDs by silica gel column chromatography.

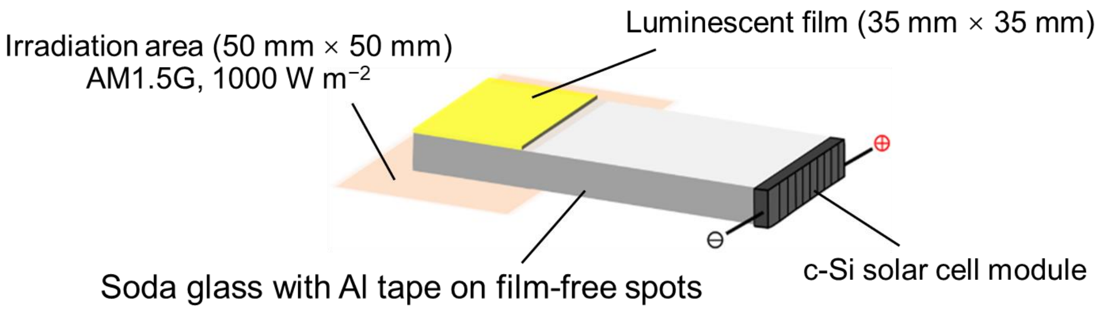

Fig. S4 Evaluation of LSC device with CDs@EVA films.

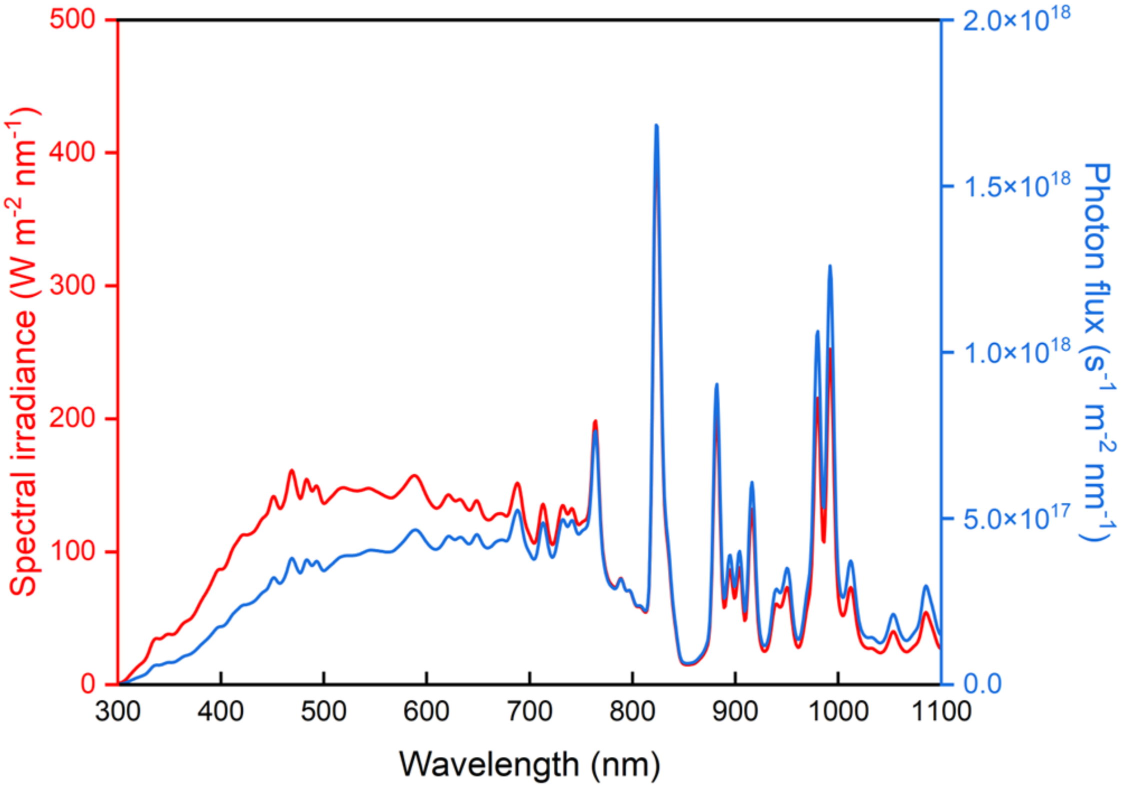

Fig. S5 Change in spectral irradiance (red) and photon flux (blue) of AM1.5G simulated sunlight as a function of wavelength.

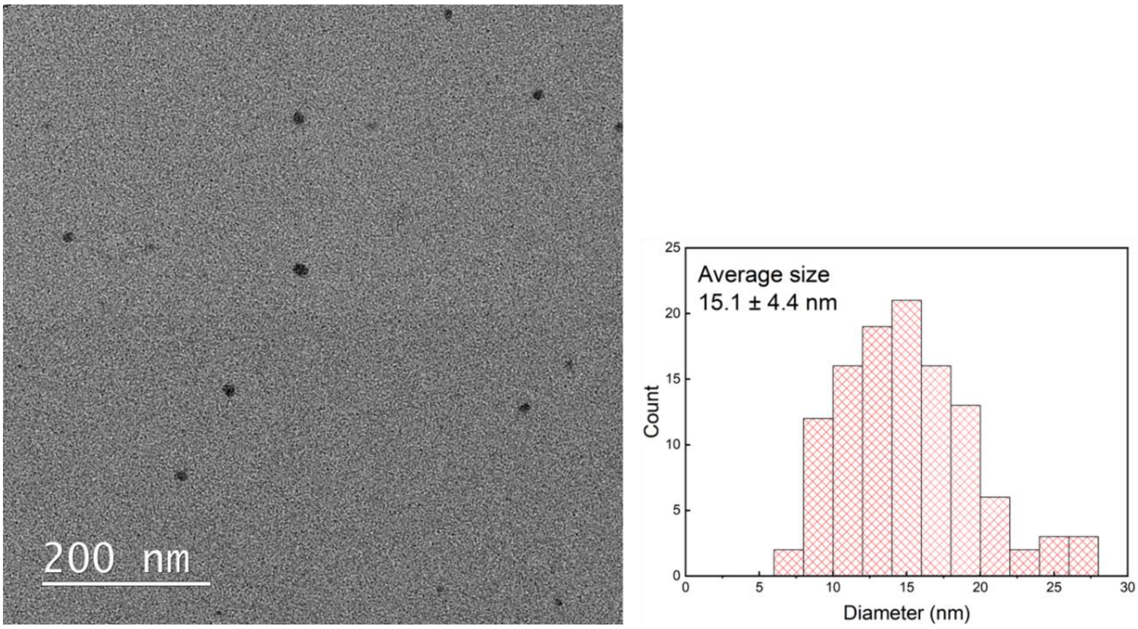

Fig. S6 FE-TEM image of purified CDs and their size distribution.

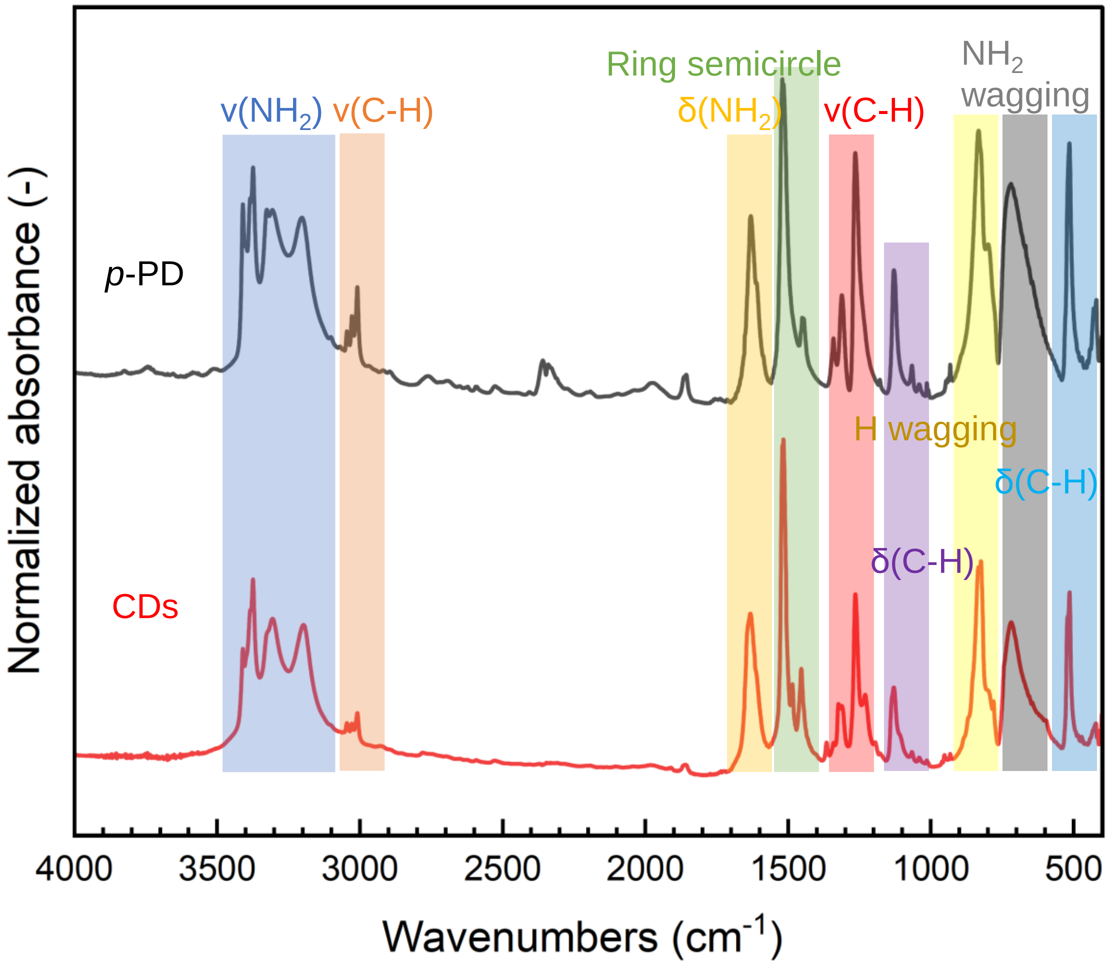

Fig. S7 FT-IR spectra of *p*-PD and purified CDs.

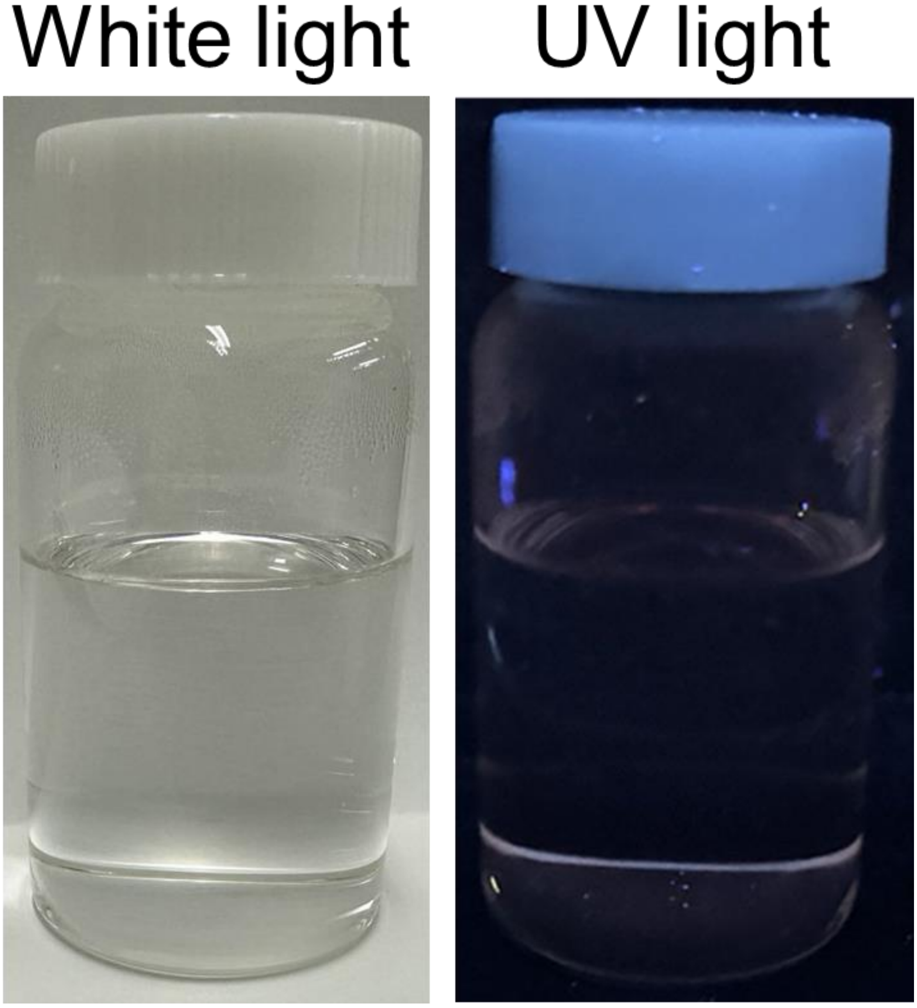

Fig. S8 Photographs of *p*-PD chloroform solution under the white light and 365 nm UV light.

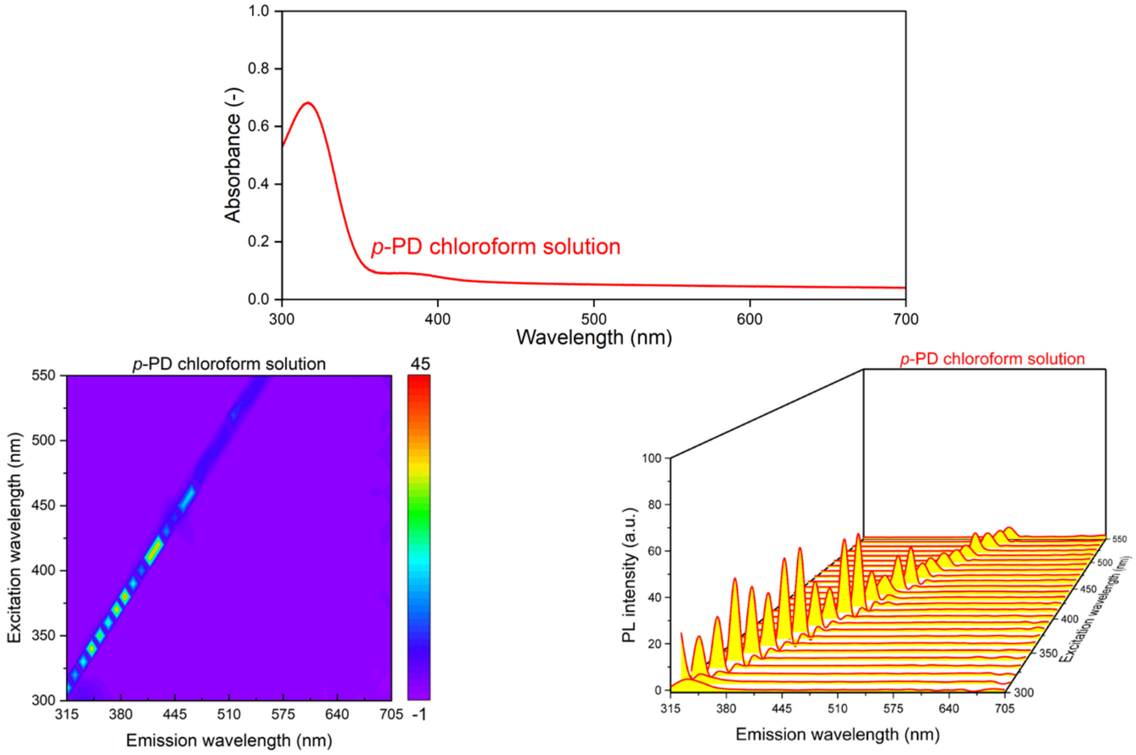

Fig. S9 UV-vis spectrum, PL/PLE mapping, and three-dimensional PL/PLE spectrum of the *p*-PD chloroform solution.

Table S2 PL/PLE properties of three different synthesized and purified CDs in chloroform.

Sample No.	λ_{ex} (nm)	λ_{em} (nm)	Storks shift (nm)	PLQY (%)
1	470	550	80	53
2	470	549	79	60
3	470	550	80	55
Average	470	550	80	56

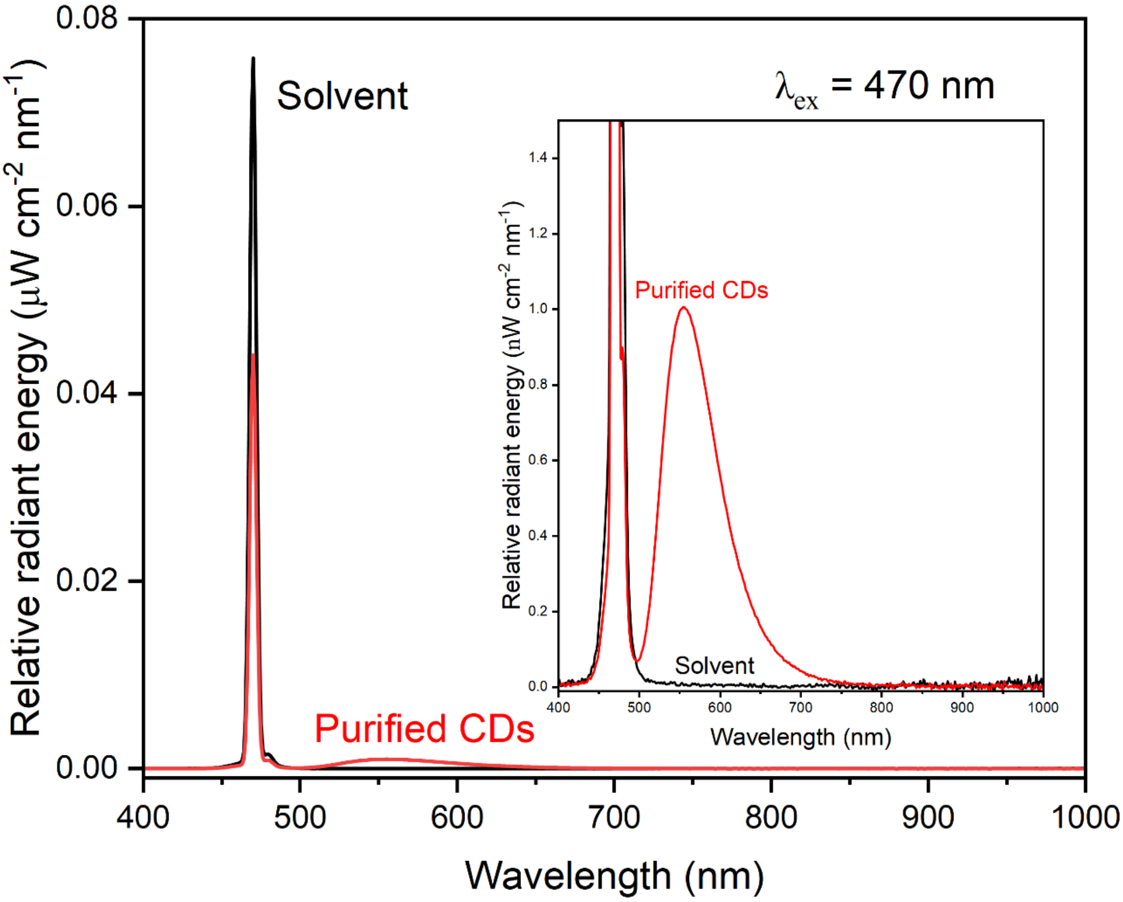

Fig. S10 PL spectra for evaluating the PLQY of the purified CDs in chloroform.

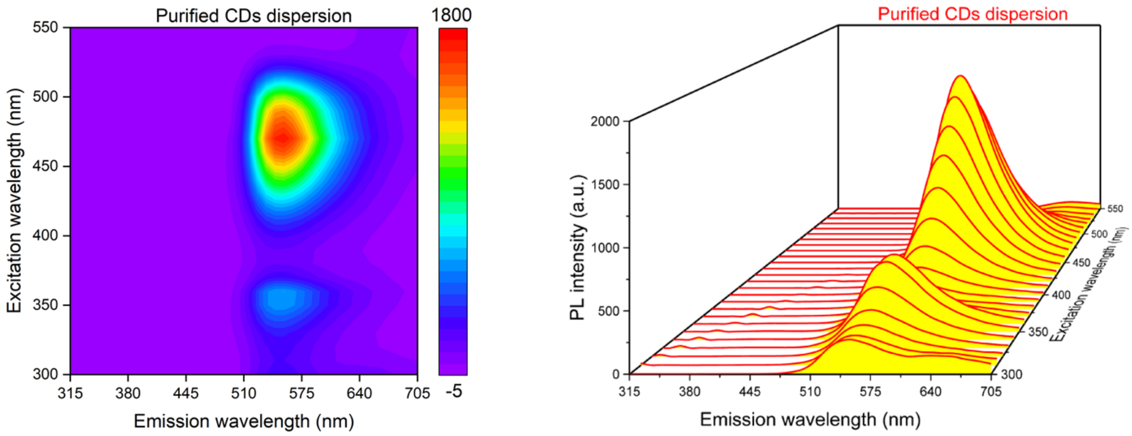

Fig. S11 PL/PLE mapping and three-dimensional PL/PLE spectra of the purified CDs in chloroform.

Table S3 The used volumes of EVA solution containing CDs, film thicknesses, emission peak wavelengths, λ_{em}, and PLQYs for the films with different CD concentrations.

Sample name	CD concentration (wt%)	Volume (mL)	Film thickness (μm)	λ_{em} (nm)	PLQY (%)
EVA	0.00	5	148 ± 2	-	-
CDs@EVA #1	0.05	5	140 ± 2	493	56
CDs@EVA #2	0.05	10	275 ± 1	493	50
CDs@EVA #3	0.05	15	408 ± 2	493	49
CDs@EVA #4	0.05	20	488 ± 3	493	49
CDs@EVA #5	0.10	5	132 ± 2	490	39
CDs@EVA #6	0.10	10	294 ± 3	490	36
CDs@EVA #7	0.10	15	421 ± 4	490	35
CDs@EVA #8	0.15	5	137 ± 2	486	35
CDs@EVA #9	0.15	10	283 ± 2	486	32
CDs@EVA #10	0.15	15	409 ± 3	486	30

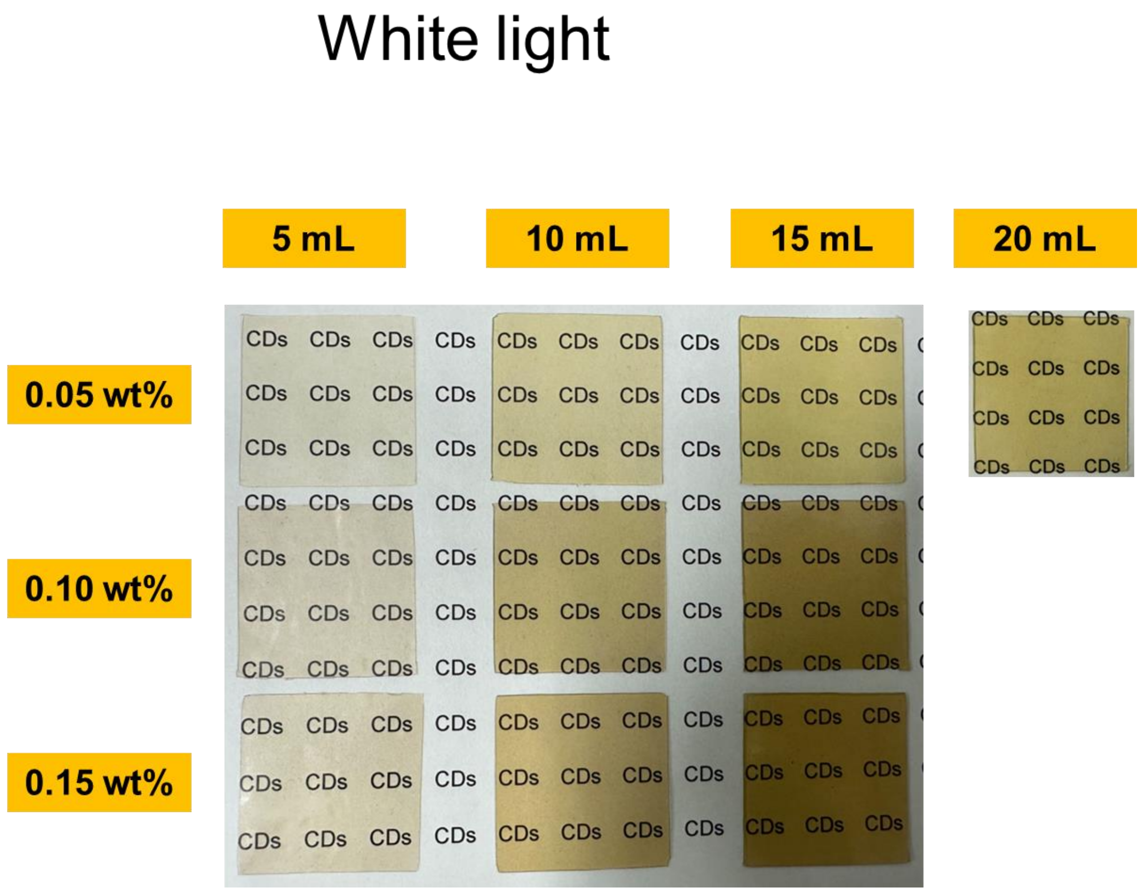

Fig. S12A Photographs of CDs@EVA films with different CD concentrations and thicknesses under white light.

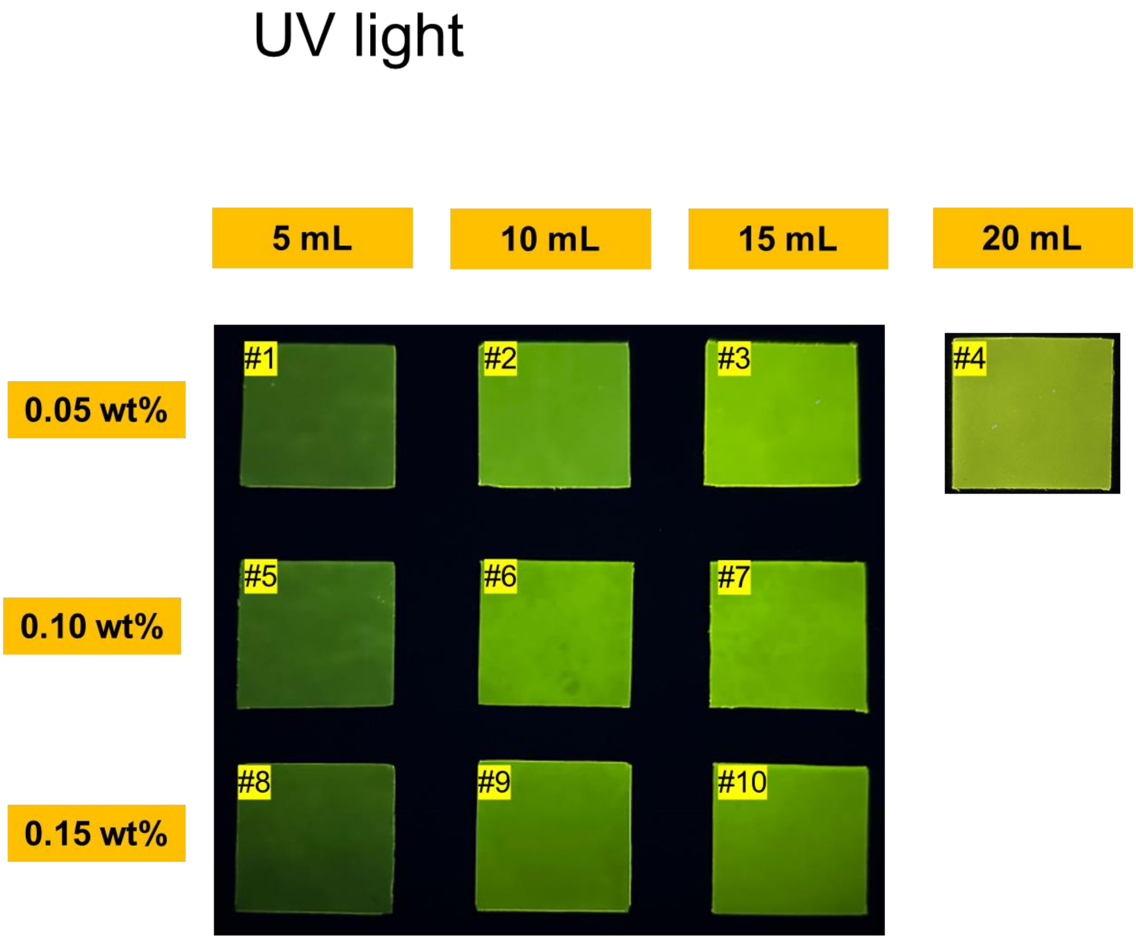

Fig. S12B Photographs of CDs@EVA films with different CD concentrations and thicknesses under 365 nm UV light.

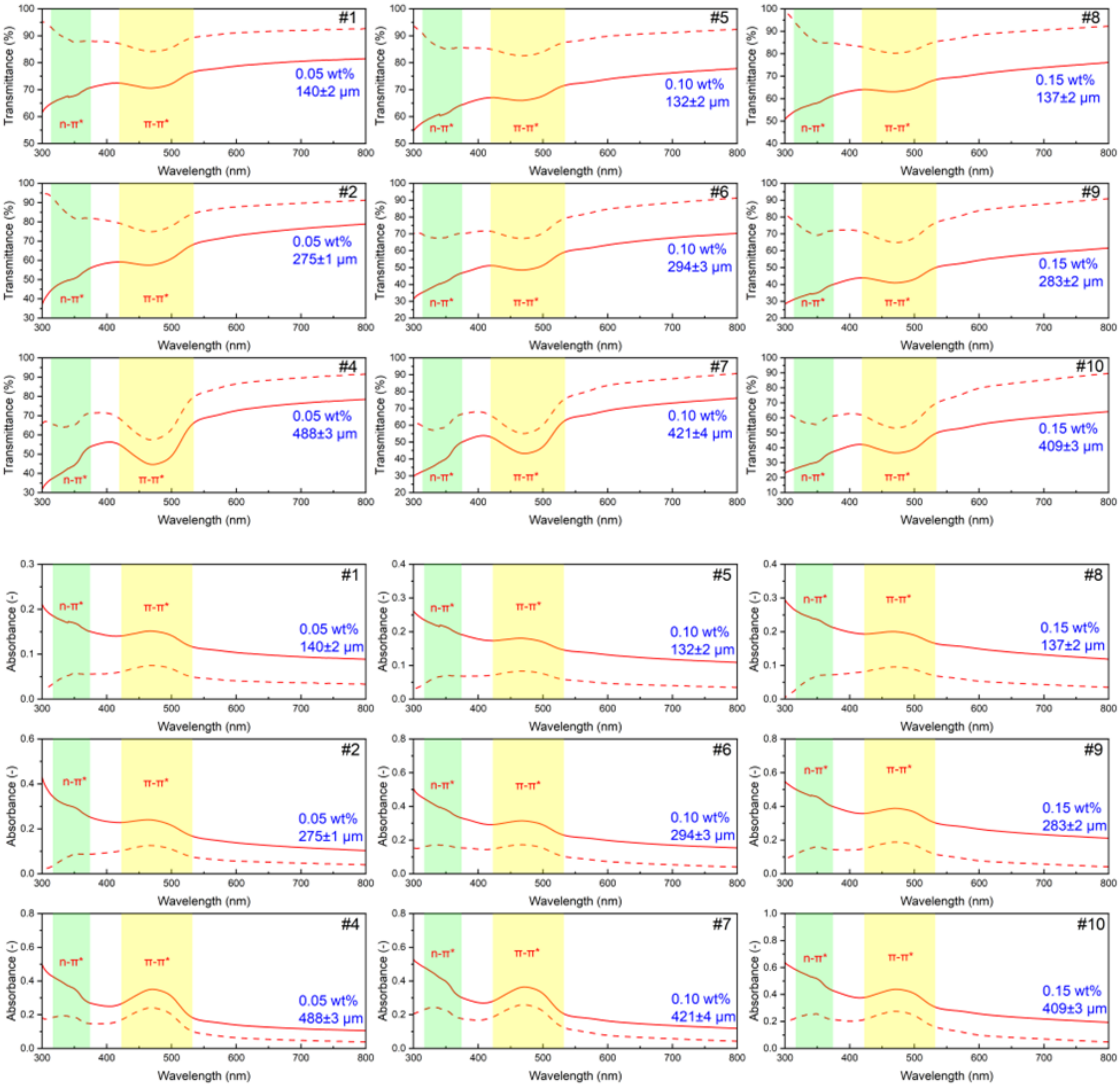

Fig. S13 In-line transmission (solid lines) and total transmission (dashed lines) spectra, and in-line absorbance (solid lines) and total absorbance (dashed lines) spectra of EVA and CDs@EVA films with different CD concentrations and thicknesses.

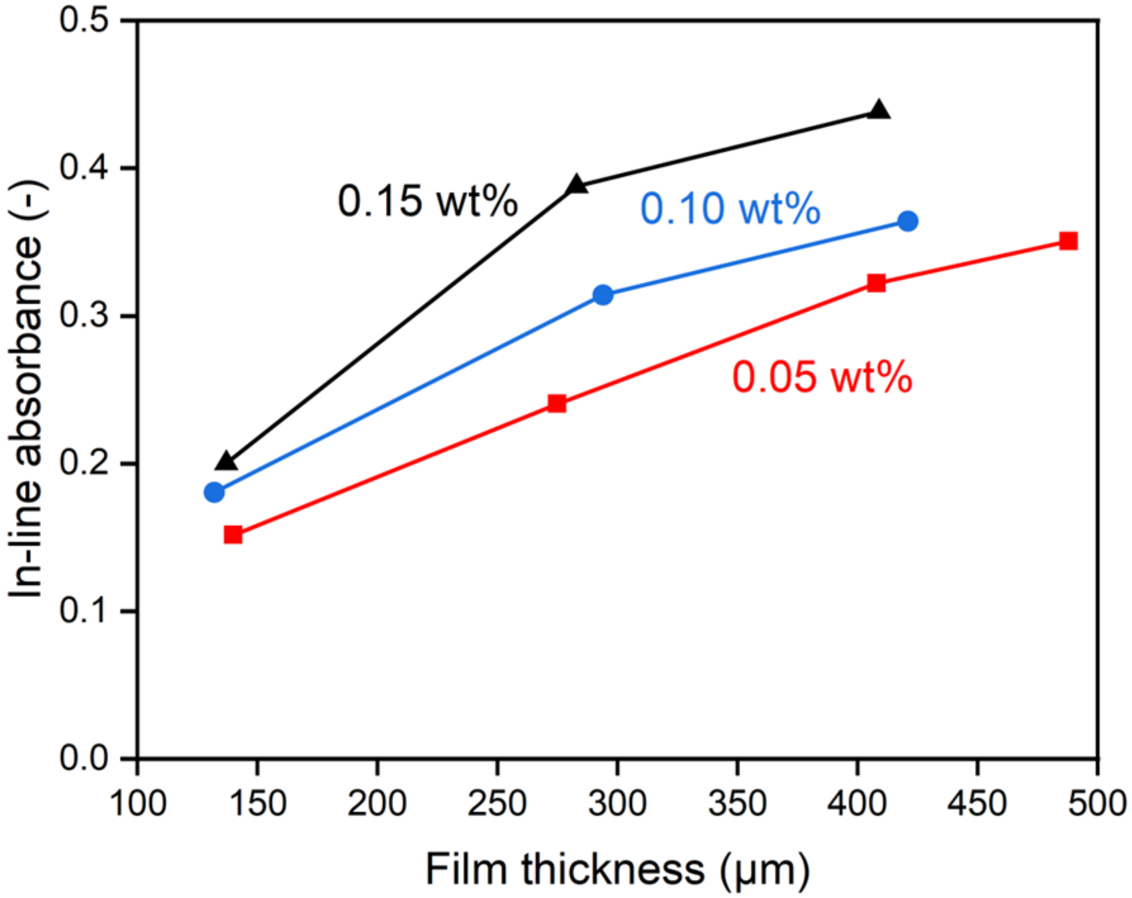

Fig. S14 Change in in-line absorbance of CD@EVA films with different CD concentrations (0.05 wt%, 0.10 wt%, and 0.15 wt%) as a function of film thickness.

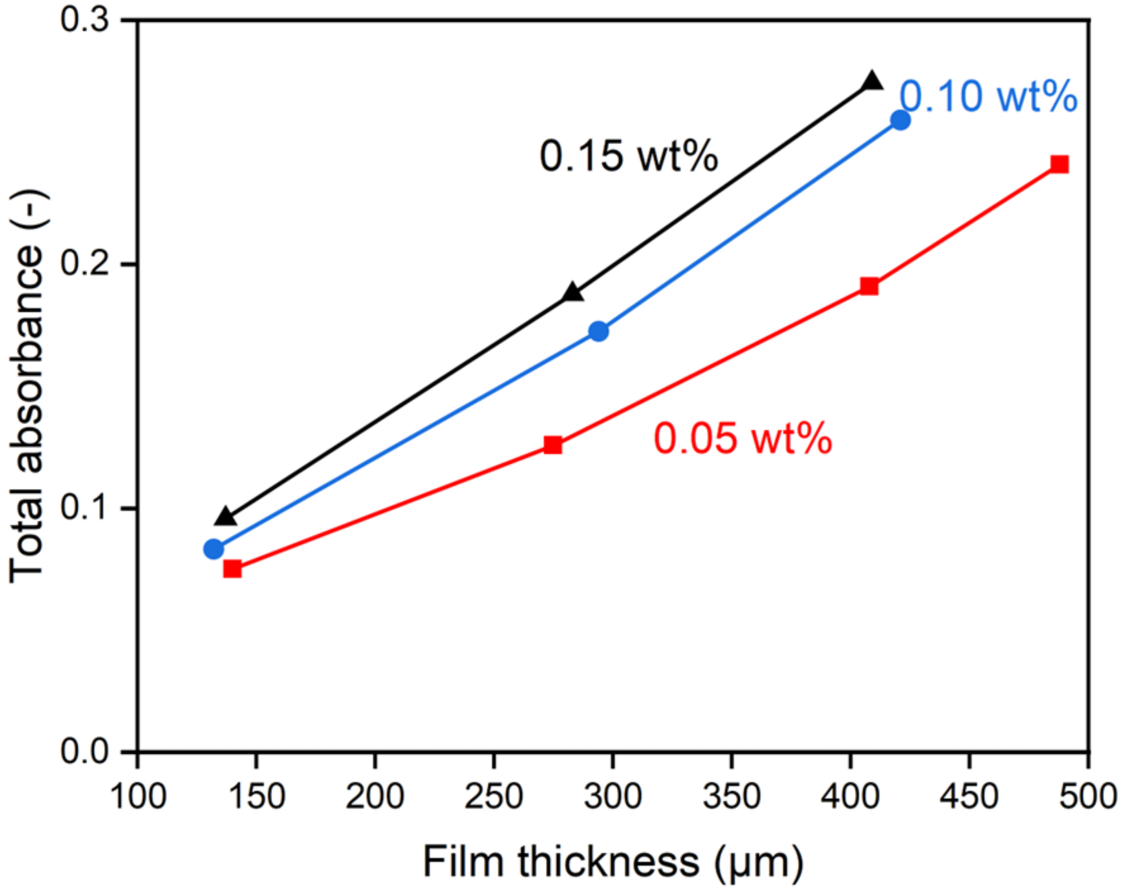

Fig. S15 Change in total absorbance of CD@EVA films with different CD concentrations (0.05 wt%, 0.10 wt%, and 0.15 wt%) as a function of film thickness.

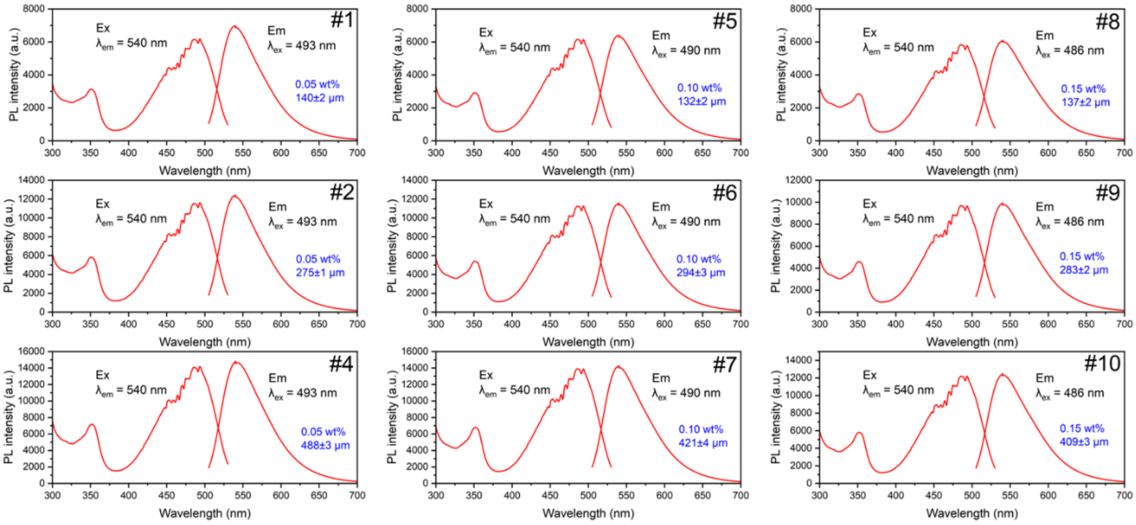

Fig. S16 PL and PLE spectra of CDs@EVA films with different CD concentrations and thicknesses.

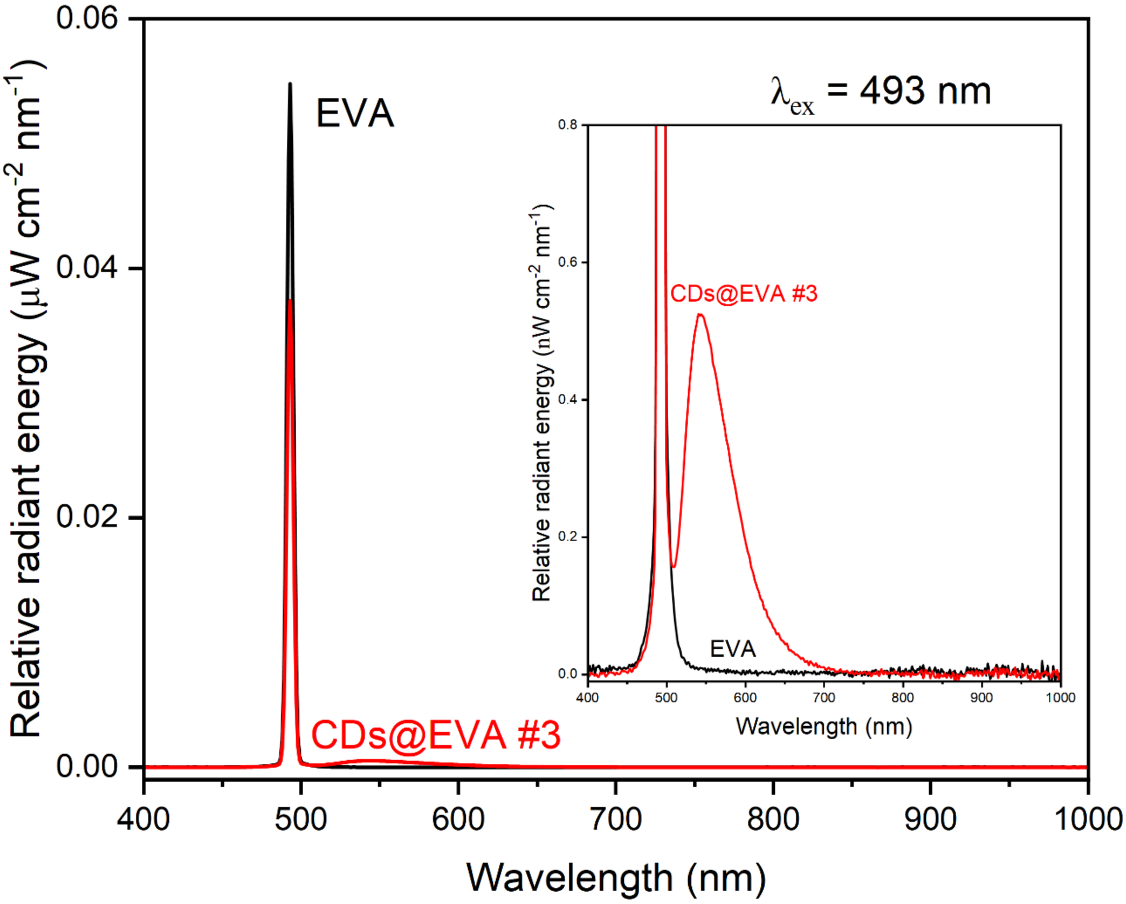

Fig. S17 PL spectra for evaluating the PLQY of CDs@EVA #3 film.

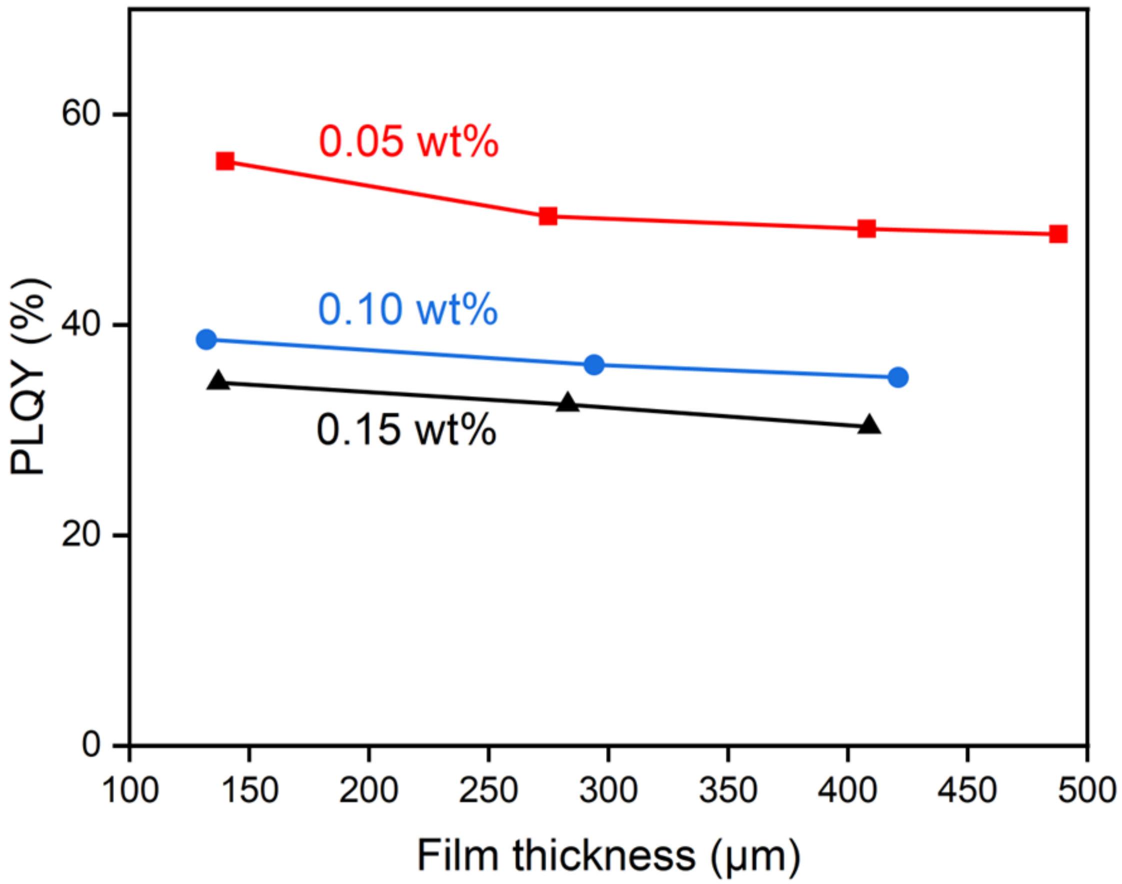

Fig. S18 Change in PLQYs of CD@EVA films with varying CD concentrations (0.05 wt%, 0.10 wt%, and 0.15 wt%) as a function of film thickness.

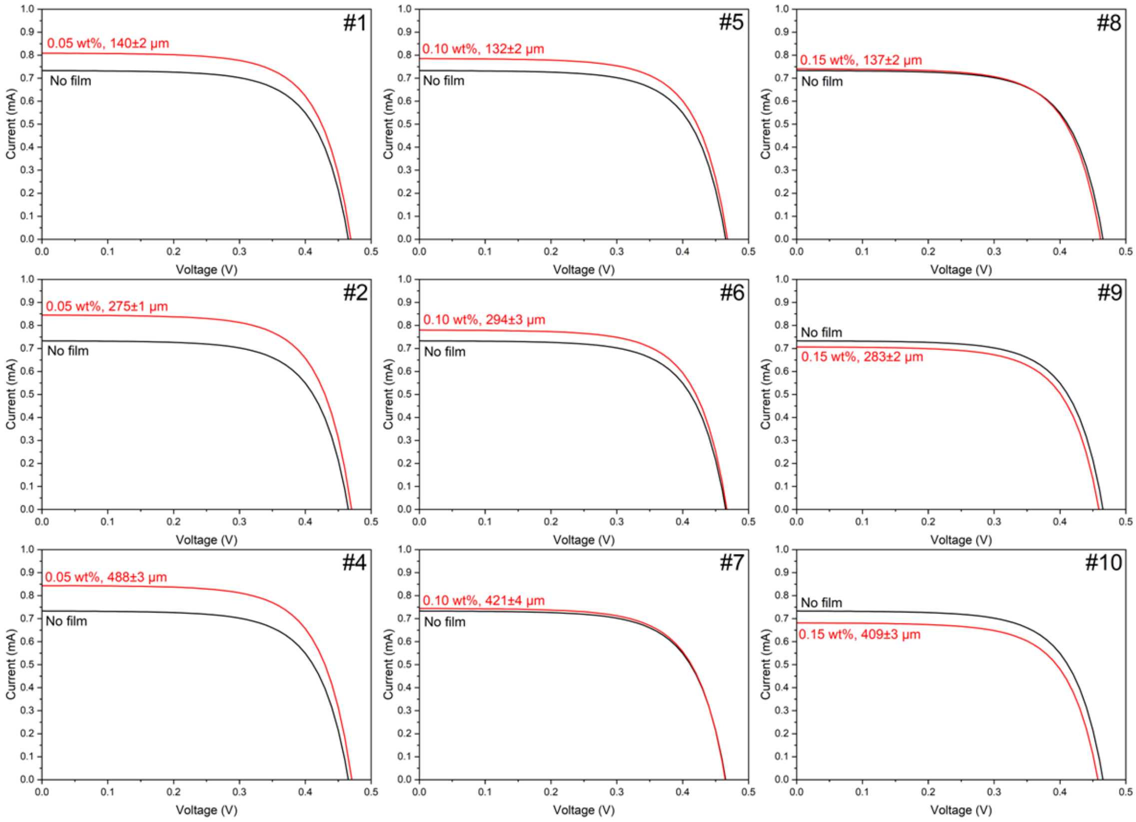

Fig. S19 *I*-*V* curves of CDs@EVA films with different CD concentrations and thicknesses.

Table S4 Results of *I*–*V* curve measurements for LSC applications

Sample	I_{sc} (mA)	V_{oc} (V)	*FF*	η (%)
No film	0.733±0.0004	0.465±0.00026	0.684±0.0007	0.0190±0.00001
EVA	0.774±0.0006	0.465±0.00004	0.684±0.0005	0.0202±0.00004
CDs@EVA #1	0.809±0.0071	0.469±0.00026	0.686±0.0004	0.0212±0.00020
CDs@EVA #2	0.845±0.0094	0.470±0.00064	0.688±0.0019	0.0223±0.00031
CDs@EVA #3	0.855±0.0092	0.471±0.00064	0.688±0.0013	0.0226±0.00031
CDs@EVA #4	0.843±0.0091	0.471±0.00038	0.688±0.0013	0.0223±0.00030
CDs@EVA #5	0.785±0.0035	0.468±0.00064	0.685±0.0013	0.0206±0.00015
CDs@EVA #6	0.780±0.0043	0.467±0.00059	0.685±0.0021	0.0204±0.00019
CDs@EVA #7	0.745±0.0048	0.465±0.00057	0.683±0.0012	0.0193±0.00018
CDs@EVA #8	0.740±0.0045	0.462±0.00010	0.681±0.0006	0.0190±0.00013
CDs@EVA #9	0.706±0.0048	0.459±0.00025	0.679±0.0012	0.0180±0.00016
CDs@EVA #10	0.682±0.0033	0.458±0.00019	0.678±0.0010	0.0173±0.00011

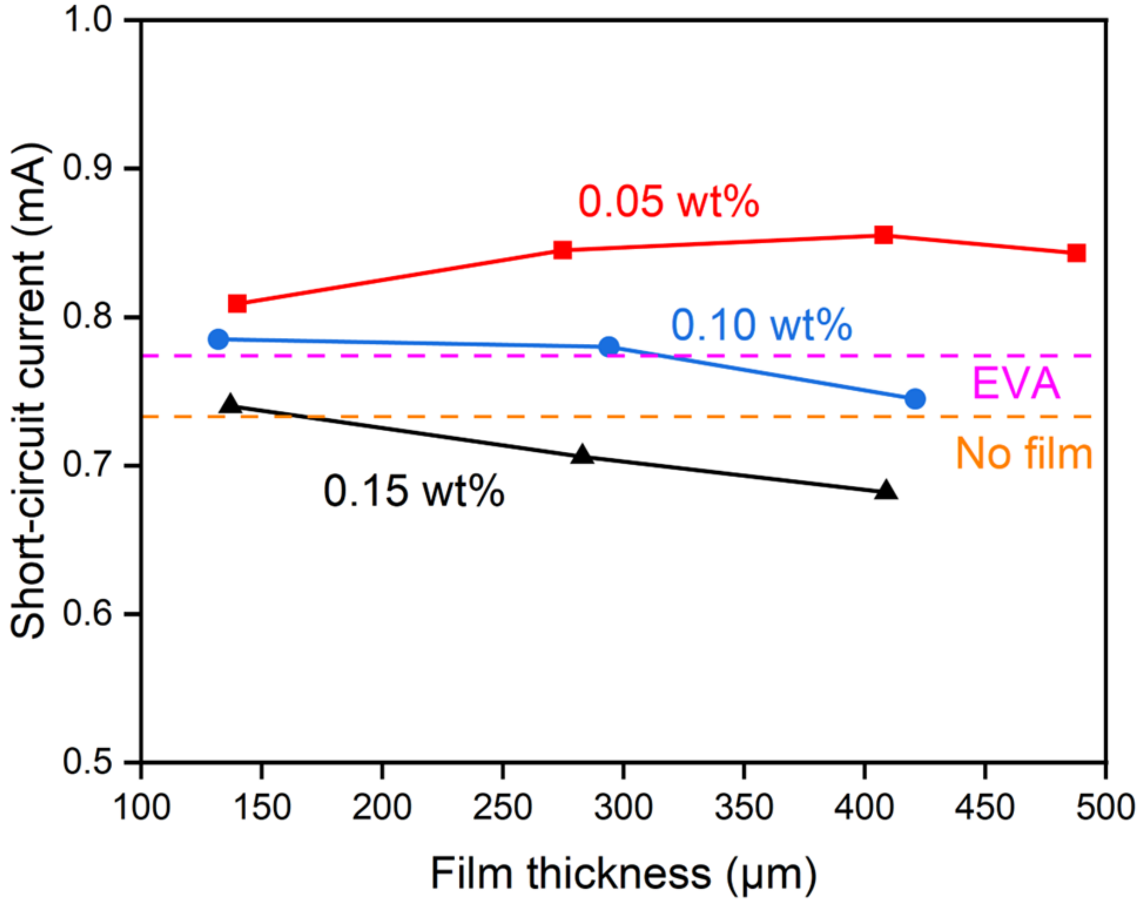

Fig. S20 Change in short-circuit currents of CD@EVA films with varying CD concentrations (0.05 wt%, 0.10 wt%, and 0.15 wt%) as a function of film thickness. Dashed lines represent reference values for no film and EVA film.

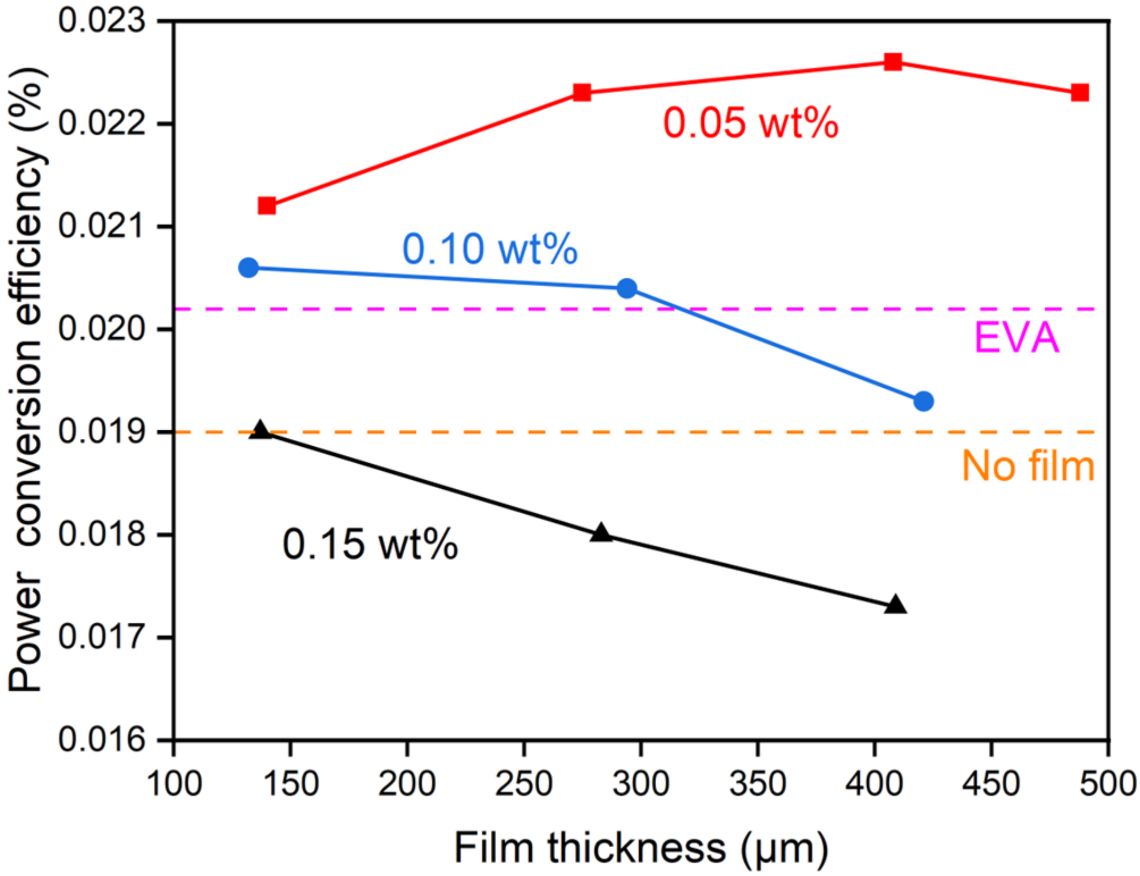

Fig. S21 Change in η of CD@EVA films with different CD concentrations (0.05 wt%, 0.10 wt%, and 0.15 wt%) as a function of film thickness. Dashed lines represent reference values for no film and EVA film.

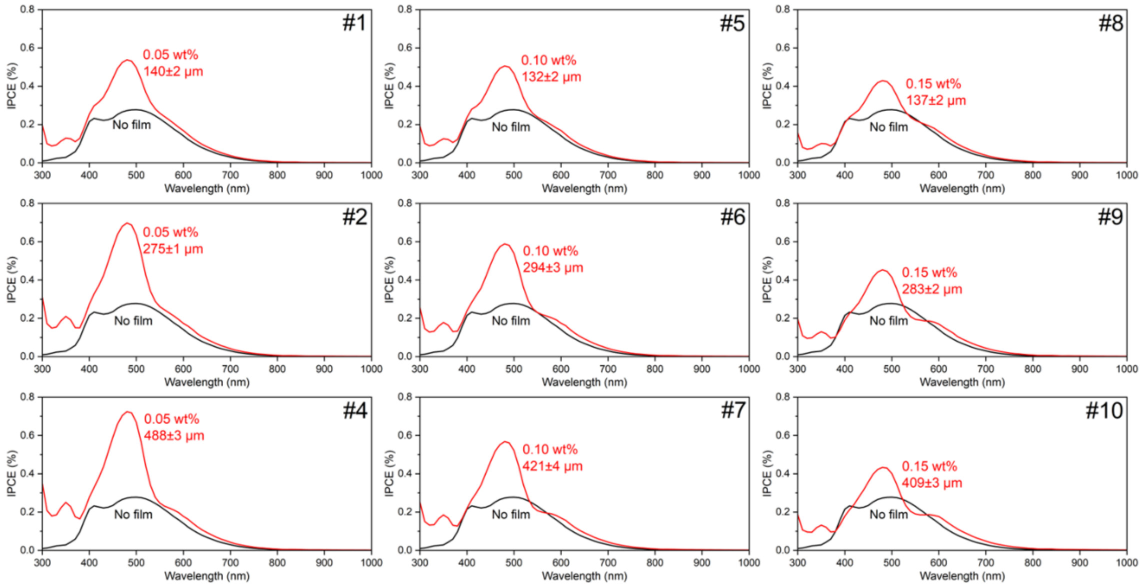

Fig. S22 IPCE spectra of CDs@EVA films with different CD concentrations and thicknesses.

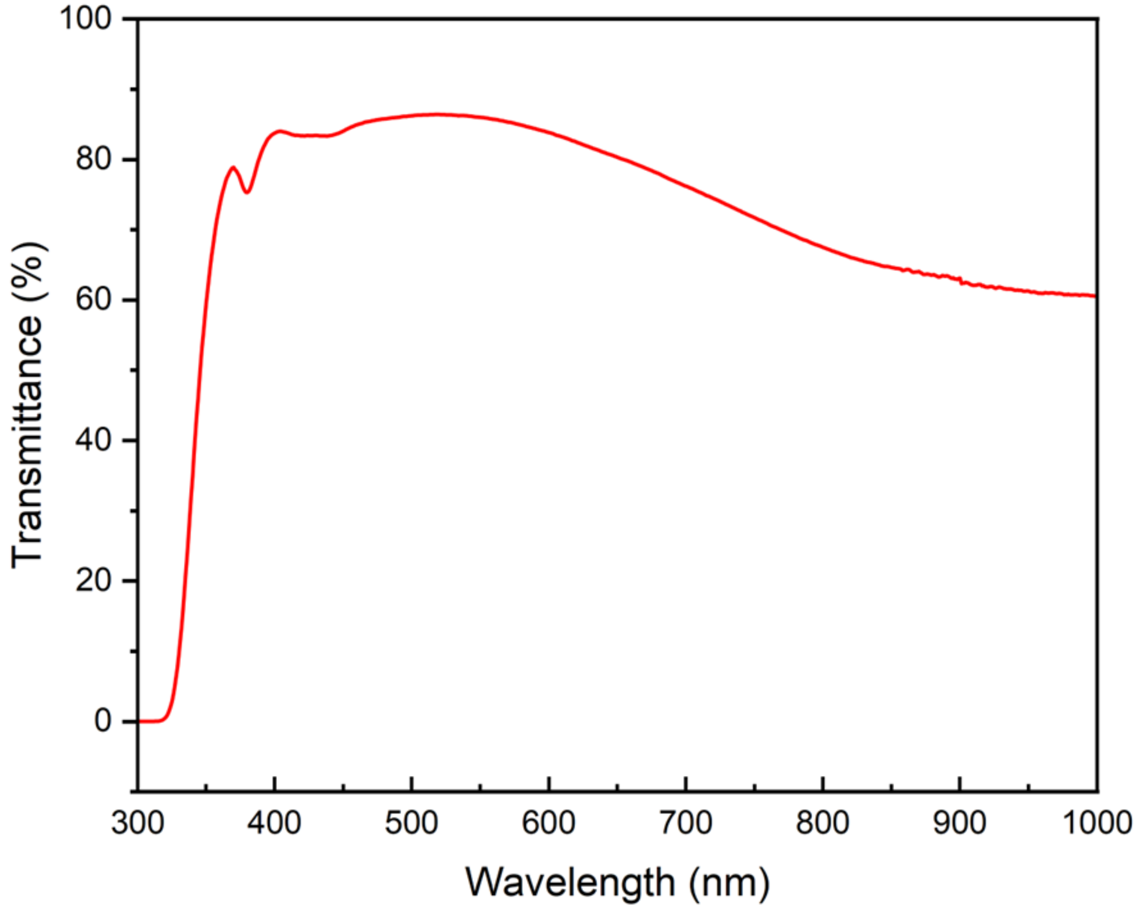

Fig. S23 Transmission spectrum of soda glass plate (10 mm thickness).

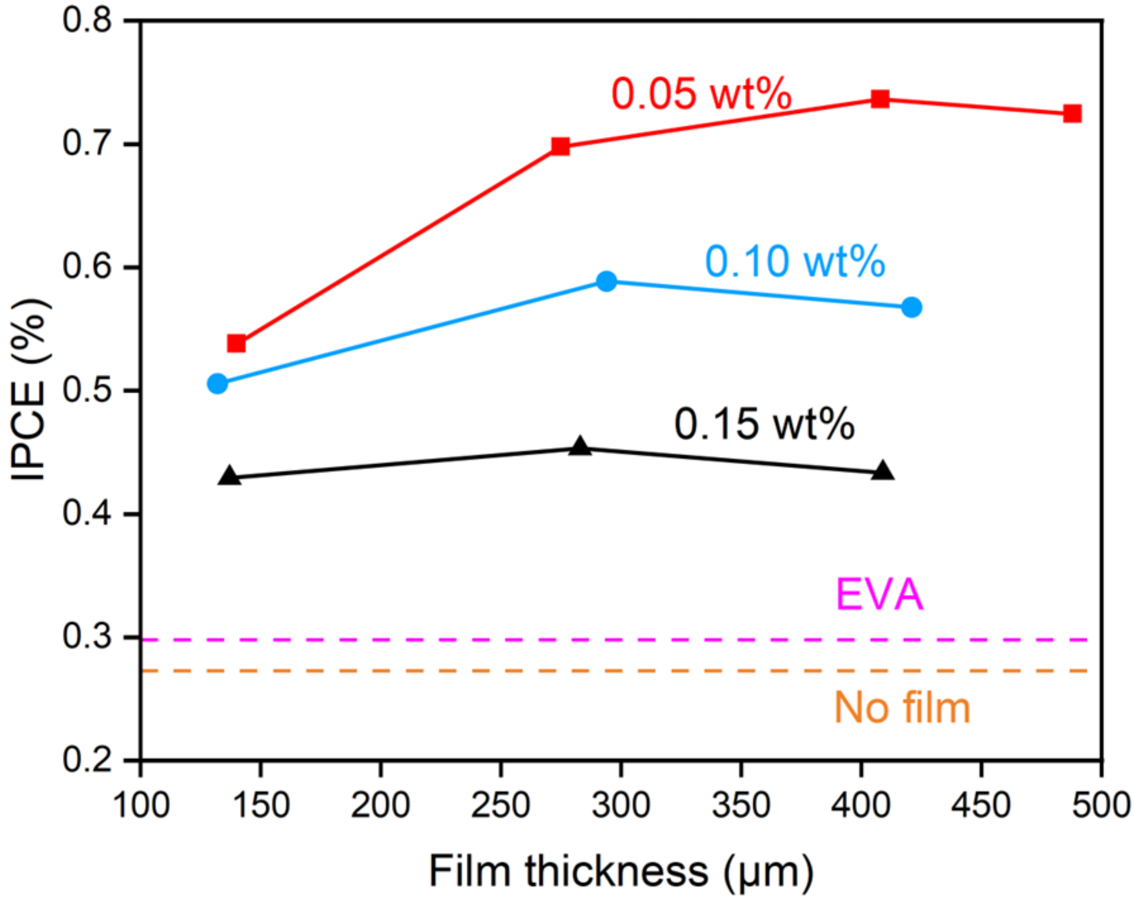

Fig. S24 Change in maximum IPCE values of CD@EVA films with different CD concentrations (0.05 wt%, 0.10 wt%, and 0.15 wt%) as a function of film thickness. Dashed lines represent reference values for no film and EVA film.

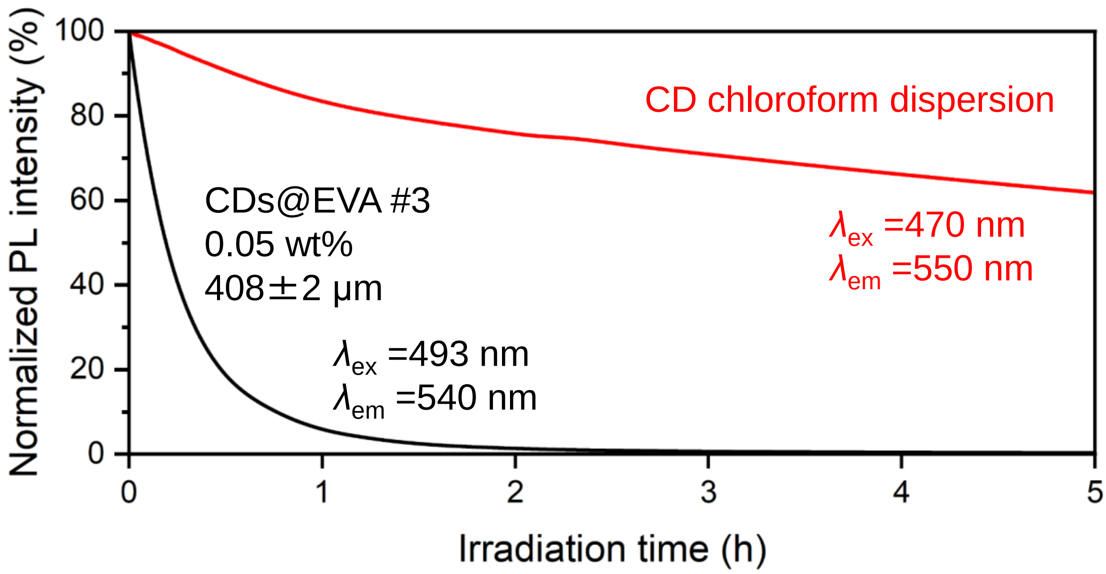

Fig. S25 Change in PL intensity of CD chloroform dispersion and CDs@EVA #3 film under the continuous optimal excitation.

References

S1 Y. Zhou, D. Benetti, X. Tong, L. Jin, Z. M. Wang, D. Ma, H. Zhao and F. Rosei, *Nano Energy*, 2018, **44**, 378-387.

S2 J. Li, H. Zhao, X. Zhao and X. Gong, *Nanoscale*, 2021, **13**, 9561-9569.

S3 Y. Wu, Y. Zhan, W. Xin, W. Cao, J. Li, M. Chen, X. Jiang, J. Wang and Z. Sun, *ACS Appl. Energy Mater.*, 2022, **5**, 1781-1792.

S4 Y. Li, P. Miao, W. Zhou, X. Gong and X. Zhao, *J. Mater. Chem. A*, 2017, **5**, 21452-21459.

S5 Z. Wang, X. Zhao, Z. Guo, P. Miao and X. Gong, *Org. Electron.*, 2018, **62**, 284-289.

S6 G. Liu, M. Zavelani-Rossi, G. Han, H. Zhao and A. Vomiero, *J. Mater. Chem. A*, 2023, **11**, 8950-8960.

S7 W. Li, X. Wang, J. Lin, X. Meng, L. Wang, M. Wang, Q. Jing, Y. Song, A. Vomiero and H. Zhao, *Nano Energy*, 2024, **122**, 109289.

S8 J. Lin, L. Wang, Q. Jing and H. Zhao, *Chem. Eng. J.*, 2024, **481**, 148441.

S9 H. Zhao, G. Liu, S. You, F. V. Camargo, M. Zavelani-Rossi, X. Wang, C. Sun, B. Liu, Y. Zhang and G. Han, *Energy Environ. Sci.*, 2021, **14**, 396-406.